

Entropy- and flow- induced superfluid states

Johan Carlström¹, and Egor Babaev^{1,2}

¹ *Department of Theoretical Physics, The Royal Institute of Technology, Stockholm, SE-10691 Sweden*

² *Department of Physics, University of Massachusetts Amherst, MA 01003 USA*

(Dated: December 3, 2024)

Normally the role of phase fluctuations in superfluids and superconductors is to drive a phase transition to the normal state. This happens due to proliferation of topologically nontrivial phase fluctuations in the form of vortices. Here we discuss a class of systems where, by contrast, non-topological phase fluctuations can produce superfluidity.

The phase transition from superfluid to normal state is driven by phase fluctuations. Remarkably, in context of superfluids it was first conjectured by Onsager¹ that the phase fluctuations responsible for the superfluid-to-normal phase transition are associated with the proliferation of vortex loops. Due to phase winding around a vortex, the presence of macroscopically large proliferated vortex loops disorders the phase $\varphi(\mathbf{r})$ of the complex order parameter fields $\psi(\mathbf{r}) = |\psi(\mathbf{r})|e^{i\varphi(\mathbf{r})}$, leading to restoration of the $U(1)$ symmetry so that $\langle |\psi(\mathbf{r})|e^{i\varphi(\mathbf{r})} \rangle = 0$. This situation also takes place in $U(1)$ type-II superconductors, as was established by Dasgupta and Halperin. The only principal difference is that the phase field in this case is coupled to vector potential \mathbf{A} , making the $U(1)$ symmetry local. In that case proliferation of vortex loops restores the local $U(1)$ symmetry via so called inverted-XY transition. In recent decades these phase transitions were investigated in great detail²⁻⁵.

In two dimensions, spin-wave-like phase fluctuations play a relatively more important role: At any finite temperature they lead to algebraic decay of correlations and thus to restoration of $U(1)$ symmetry⁶. However it requires proliferation of topological defects (vortex-antivortex pairs) to make correlations short range via the Berezinskii-Kosterlitz-Thouless transition⁷⁻⁹.

In multi-component systems, phase fluctuations in the form of composite vortices generally results in the formation of paired states¹⁰⁻¹². However these fluctuations still act to destroy superfluidity, albeit in some non-trivial channels.

The question which we raise in this work is: are there situations where fluctuations *induce* superfluidity or superconductivity rather than destroy it? I.e. if a situation can arise where a system posses a channel that is not superfluid or superconducting in the ground state, but fluctuations cause the system to exhibit superfluidity in this channel at, for example, elevated temperature. We argue that indeed (quasi-)superfluid states can be generated for entropic reasons due to phase fluctuations.

Often the superfluid phase transition is associated with a spontaneous breakdown of $U(1)$ symmetry. Superfluidity can indeed arise without a symmetry breaking like in the aforementioned two dimensional case at finite temperature, or the one dimensional case at zero temperature. Superfluidity can in principle exist in macroscopic systems that explicitly break $U(1)$ symmetry, although only weakly, thus allowing "pseudo" Goldstone bosons. In such a case the macroscopically large system can still be superfluid. Here we especially

focus on a further possible generalisation where a superfluid mode can be associated with a $U(1)$ -like degeneracy (or near-degeneracy) not corresponding to a $U(1)$ symmetry of the effective potential. In general, phase fluctuations and even vortices can originate from this degeneracy.

In the scenario which we discuss here, a superfluid system when heated goes into an entropically-induced state where an additional superfluid channel is opened. We also consider entropically induced states that are not associated with additional superfluid channels, but posses properties different from those of the ground state.

Here we discuss certain multicomponent models because of the substantial progress in creation and investigation of these systems recently.

In the cold atoms field, interest is driven by the extensive possibilities to realise multicomponent superfluid states. These systems allow high precision tuning of various forms of inter-component interactions. In the context of superconductivity, the interest was driven recently by discoveries of superconductors with complicated multi-band order parameters.

An illustrative formalism to discuss in the context of multicomponent condensates is the multicomponent Ginzburg-Landau (GL) functional. We start the discussion with this functional, although our results do not rely on the existence of the GL expansion in the sense that the effective potential does not have to be represented in this particular form of series in powers of ψ_i . The free energy density is given by

$$F = \sum_i \frac{1}{2} |\nabla \psi_i|^2 + \sum_{i,j} \eta_{ij} \psi_i \psi_j^* + \sum_{i,j,k,l} \nu_{ijkl} \psi_i \psi_j \psi_k^* \psi_l^*, \quad (1)$$

where summation is conducted over N components (complex fields ψ_i). These components can originate from Cooper pairing in different bands or Josephson-coupled superconducting layers or correspond to different components of Bose condensed cold atoms. The intercomponent interaction terms in (1) make up the first- and second- order Josephson couplings. Such couplings can be realised in Josephson-coupled multilayers and Josephson-junction arrays where couplings can in principle be controlled. Intercomponent couplings of this kind can also be realised in cold atoms.

In the simplest case the mixed bi-quadratic terms of the form $\psi_i \psi_j^* + c.c. = |\psi_i| |\psi_j| \cos(\varphi_i - \varphi_j)$ lock phase differences and explicitly break the symmetry down to $U(1)$, which

is then associated with the total phase sum. However, these terms do not necessarily break the symmetry completely. For example in the $N = 3$ case, even retaining only leading order couplings can lead to $U(1) \times Z_2$ broken symmetry^{13–17}. Higher order couplings are important for example in dirty superconductors (see e.g.¹⁸), but may also have different origin. This problem becomes even richer in the four component case, with features such as a variety of accidental degeneracies¹⁶ appearing even at the level of only bilinear couplings.

One possible property of the free energy (1) is the existence of local minima of the free energy. This feature is quite generic and is present also in the London model. Consider a three-component lattice London model containing only phases, and that exhibits a set of phase-locking terms:

$$H = - \sum_{i=1}^3 \sum_{\langle j,k \rangle} \cos(\varphi_{i,j} - \varphi_{i,k}) \quad (2)$$

$$+ \sum_k V(\varphi_{12,k}, \varphi_{13,k}), \quad \varphi_{ij,k} = \varphi_{j,k} - \varphi_{i,k} \quad (3)$$

The first term describes gradient energy and contains a summation over i , which denotes the superconducting components, and $\langle j,k \rangle$ which are all nearest neighbours. The second term contains a summation of k over all lattice points and describes the potential energy. We will consider three examples of different potentials which are constructed to represent minimalistic models of the situations mentioned above, with local minima in the free energy landscape. The potentials are chosen so that they lock phase differences, explicitly breaking the symmetry down to $U(1)$. In the ground state this symmetry is broken spontaneously. The local minima correspond to a different phase locking pattern with slightly higher energy.

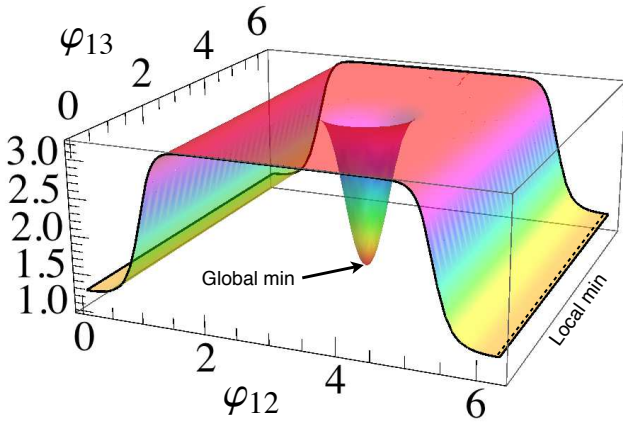


Figure 1. The potential (1) exhibits a global min in $\varphi_{12} = \varphi_{13} = \pi$ and a local min corresponding to $\varphi_{12} = 0$. The potential is given by $V_1(\varphi_{12}, \varphi_{13}) = \tanh(3 - 5 \cos \varphi_{12}) + 2.2 \tanh(8 \cos \varphi_{12} + 8 \cos \varphi_{13} + 16)$

The potentials are displayed and defined in Fig. 1,2,3. Two of them, V_1 and V_2 , are specifically constructed as archetypical representations of two kinds of energy landscapes with strong features that facilitate numerical study, while V_3 is built from interaction terms of the form $\psi_i^* \psi_j$ and $\psi_i^* \psi_j^* \psi_k \psi_l$

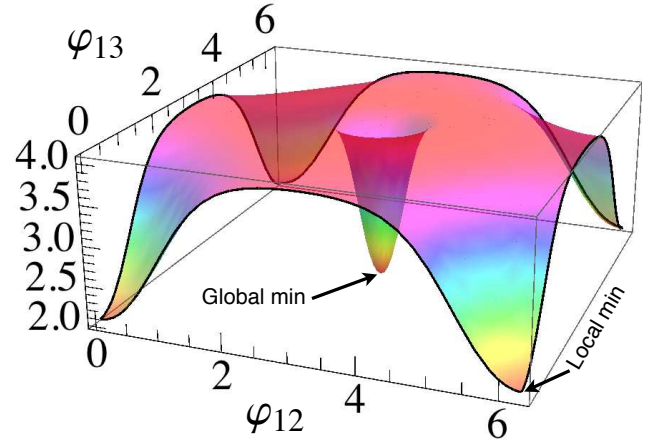


Figure 2. The potential (2) possesses minima in the form of two wells: One deep but narrow situated in $\varphi_{12} = \varphi_{13} = 0$ and a slightly more shallow, though wider located in $\varphi_{12} = \varphi_{13} = \pi$. The potential is given by

$$V_2(\varphi_{12}, \varphi_{13}) = 2.05 \tanh(8 \cos \varphi_{12} + 8 \cos \varphi_{13} + 16) + 2 \tanh(2 - \cos \varphi_{12} - \cos \varphi_{13}).$$

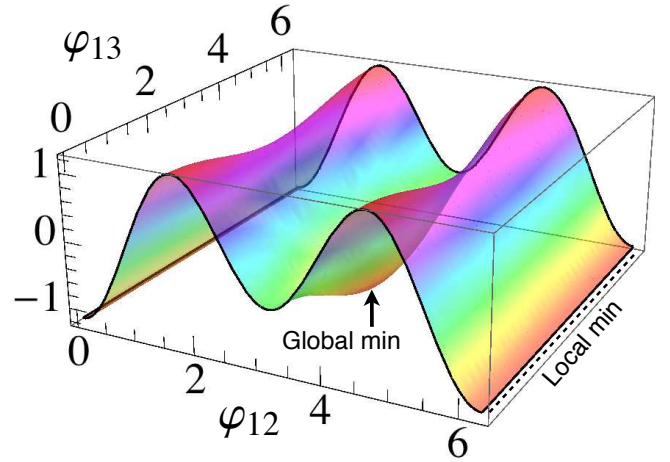


Figure 3. The potential (3) possesses a global min in $\varphi_{12} = \varphi_{13} = \pi$ and a local min corresponding to $\varphi_{12} = 0$. The potential is given by $V_3(\varphi_{12}, \varphi_{13}) = -\cos 2\varphi_{12} - 0.18 \cos \varphi_{12} + 0.2(1 - \cos \varphi_{12}) \cos \varphi_{13}$.

which constitute the first and second order Josephson harmonics, and so the potential V_3 can be constructed at the level of quadratic and quartic Josephson terms in the context of GL theory.

Creation of domain walls between the minima is generally associated with some energy that depends on the shape of the potential. If this energy is large compared to the temperature, then transitions between the states will be rare. This should give rise to two states, one that is centred around the minimum which we denote (\downarrow), and another state centred around the local minimum which we denote (\uparrow). Another feature of these potentials is that they exhibit a comparatively steep slope around the global minimum, whilst the local minimum is surrounded by a flatter slope in the energy landscape. Con-

sequently, the energy cost of phase-difference excitations is smaller in the state (\uparrow) than in (\downarrow).

We are interested in the role of phase fluctuations in these systems. The fact that these are energetically cheaper in the state (\uparrow) implies a lower free energy at a certain temperature, resulting in a transition to an entropically stabilised state. The normal role of phase fluctuations is to restore the $U(1)$ symmetry, but in the models (1,3) the situation is reversed as the state (\uparrow) actually poses an additional superfluid mode.

To investigate the entropically stabilised superfluid state we have conducted Monte Carlo simulations based on the metropolis algorithm with two types of update: The first is a local update where a single lattice point is selected and three new phases φ'_i (one for each component) are generated so that the probability density $p(\varphi'_i)$ is uniformly distributed in the interval $[0, 2\pi]$ and otherwise zero. The second is a global update where one of the phases is selected and an update is proposed so that $\varphi_i \rightarrow \varphi_i + \Delta\pi$ on all lattice points simultaneously.

The updates are accepted with probability $e^{-\beta\Delta E}$. For each model, 256 different coupling strengths (inverse temperatures) were selected. For each coupling strength, two simulations corresponding to the two possible states (\uparrow, \downarrow) were prepared. The equilibration was conducted in two stages: First, an initial 50,000 local updates were carried out (i.e. each lattice point was subject to 50,000 proposed updates). Second, another 50,000 updates were carried out. But this time, every 3 updates, a global update was proposed.

After the equilibration, data was collected as follows: Local updates were proposed 200 times for every lattice point. For every 3 such updates, a global update was proposed. Then, simulation data was collected. This process was repeated 28,000-100,000 times depending on system size, resulting in the same number of data points. The simulations were conducted on a cubic lattice with periodic boundary conditions and system sizes $8 \leq L \leq 40$. Finally, points in the parameter space where the system keeps tunnelling between the two states were discarded (this mainly occurred for smaller systems in model 3).

During the simulation several quantities were monitored: The coherence of the individual phases was measured as

$$o_\gamma(T) = \left\langle \left| \frac{1}{L^3} \sum_j e^{i\varphi_{\gamma,j}} \right| \right\rangle \quad (4)$$

where index $1 \leq \gamma \leq 3$ denotes the different phases. To identify the two states we also introduce

$$S_{12} = \langle \cos(\varphi_2 - \varphi_1) \rangle \quad (5)$$

In the state (\downarrow) we should have $S_{12} \sim -1$ while in the state (\uparrow) we expect $S_{12} \sim 1$. To determine the properties of the sector $\varphi_{1,3}$, we introduce the following two functions: When the system is in a state where φ_{13} has an appreciable mass (which turns out to be the case in model 2 but in fact also 3) we calculate

$$S_{13} = \langle \cos(\varphi_3 - \varphi_1) \rangle \quad (6)$$

which is nonzero when the mode is massive. When the mode becomes superfluid (which occurs in model 1), this is best

illustrated by the correlator

$$C_{13} = \frac{1}{N} \int dr \left[\langle X(r) \cdot X(0) \rangle - \langle X(r) \rangle \cdot \langle X(0) \rangle \right], \\ X = \{\cos \varphi_{13}, \sin \varphi_{13}\}, \quad N = L^D. \quad (7)$$

Here superfluid modes are recognised as having non-zero correlations even in large systems. Consequently, in a large system C_{13} takes a finite value in a superfluid while it approaches zero for a massive mode.

The results of the simulations are summarised in Fig. 4. All three models exhibit a transition to an entropically stabilised state that is driven by non-topological phase fluctuations. These fluctuations are energetically cheaper in the state (\uparrow), something that is reflected in the fact that the phase coherence (o_i) at a given coupling strength is smaller in this state (A-C). The transition is associated with a change of the parameter S_{12} , which is ~ -1 in the state (\downarrow) and $\sim +1$ in (\uparrow) (D).

In the model (1), the ground state (\downarrow) breaks $U(1)$ symmetry, while in the state (\uparrow), the $U(1)$ -like degeneracy is broken in addition. This is reflected in the appearance of a nonzero correlator (C_{13}) and thus entropically induced superfluidity

In the model (2), the minima are: a deep and narrow well (\downarrow) and a slightly more shallow well with a flatter slope (\uparrow) with no additional degeneracy. Thus, in this case the phase fluctuations can drive a transition between two states with different phase lockings and different length scales/masses.

The model (3) is similar to (1) in the sense that it exhibits a ground state where the energy is invariant under $U(1)$ transformations as well as a local minimum corresponding to $\varphi_{12} = 0$. In the local minimum the energy is independent of φ_{13} , implying that it has an additional degeneracy. However, in this state the energy is only independent of φ_{13} when $\varphi_{12} = 0$ exactly, i.e. precisely at the bottom of the 'valley'. At any nonzero temperature, thermal fluctuations renders this mode massive (although with a comparatively very small mass). This is reflected in the fact that S_{13} (shown in E3) is nonzero even for the state (\uparrow). At finite length scale, this state however shares properties with a $U(1) \times U(1)$ superfluid.

We note that in these types of systems, the transitions between the states can occur not only because of thermal fluctuations, but also as a result of an applied phase twist. This can be demonstrated as follows: to simplify calculations, consider a system similar to model (1), but with an infinitely narrow well. Let the energy be 0 in the well, V in the valley and U everywhere else so that $0 < V < U$. Suppose $\varphi_{1,3}$ is twisted by $N2\pi$ along a system of size L . In the state (\downarrow) the twist results in kinks of width $l_w = \pi\sqrt{2/U}$ and energy $E_w = 2\pi\sqrt{2U}$. In the state (\uparrow) the twist instead results in an evenly distributed phase gradient. The energy difference between the two solutions can then be written

$$E_\uparrow - E_\downarrow = L \left(-\rho E_w + 2\pi^2 \rho^2 + V \right), \quad \rho = \frac{N}{L}. \quad (8)$$

This expression is valid provided $0 \leq \rho \leq 1/l_w$ (since the size of the kinks is l_w). If $\rho = 0$, this is positive and (\downarrow) is the lowest energy state. Inserting $\rho = 1/l_w$ we instead obtain $E_\uparrow - E_\downarrow = V - U < 0$, and the lowest energy state

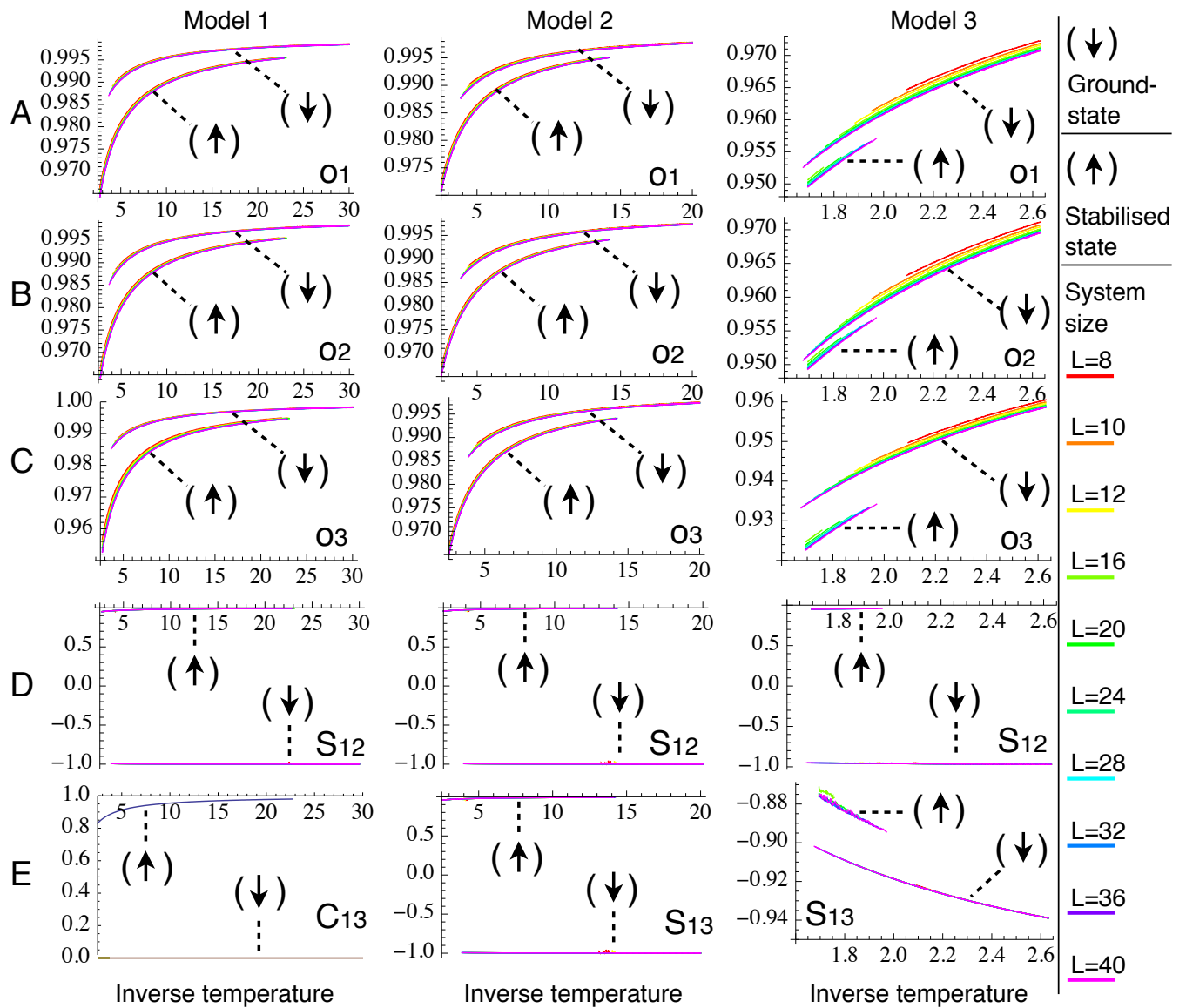


Figure 4. Summary of the simulation results. The three columns correspond to the potentials 1, 2 and 3. The first three rows (A-C) give the averages o_1 , o_2 , o_3 (4) for system sizes $8 \leq L \leq 40$. These are zero if a system is in the normal state. Row (D) gives S_{12} (5) while (E) shows the correlator C_{13} (7) for model (1) and S_{13} (6) for models (2,3). In (D,E) data is only displayed for the system size $L = 40$. In rows (A-C) the two curves correspond to the two different states $(\downarrow\uparrow)$. These two states coexist in part of the parameter range, particularly in the models (1,2), due to hysteresis.

is (\uparrow) . Thus, above some critical phase twist ρ_c , it is energetically beneficial to go to the superfluid state (\uparrow) where the system can take advantage of the (near) degeneracy in the energy landscape to distribute current. Below it, (\downarrow) becomes the preferred state.

Finally, we address the question of mass generation through thermal fluctuations.

The fact that the induced superfluid state does not correspond to an underlying symmetry of the Hamiltonian means that fluctuations can result in this mode becoming massive.

The extent to which this occurs very much depends on the shape of the potential, as well as the temperature. In the model

(3) this phenomena is directly visible even at low temperature in a finite system, where it renders S_{13} nonzero in the state (\uparrow) . In contrast, the model (1) is less affected by this process and within the accuracy of the simulations the mode is massless. When the fluctuations render the mode massive the system behaves as a superfluid on length scales smaller than the inverse mass of the mode. The Fig. 5 shows the correlator C_{13} at higher temperature for model (1) and system sizes $4 \leq L \leq 28$. At these sizes the φ_{13} -sector remains superfluid until vortex proliferation takes place at $\beta \approx 0.45$.

In conclusion we demonstrate the existence of a class of systems that posses a channel that is not superfluid in the

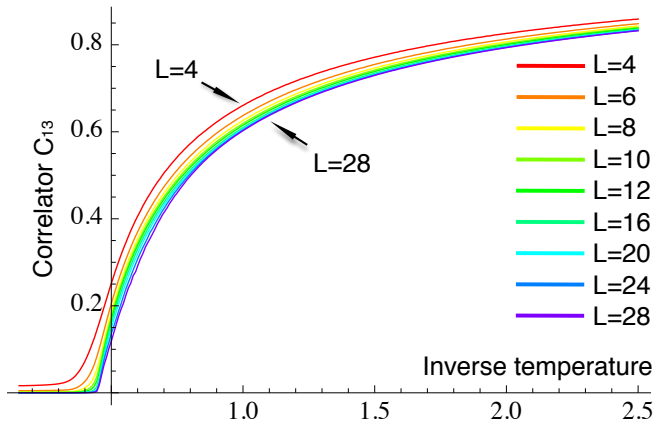


Figure 5. Correlator C_{13} for model (1) at higher temperature. System sizes range from 4 to 28. The point $\beta \approx 0.45$, where C_{13} approaches zero corresponds to the transition where superfluidity is destroyed by vortex proliferation.

ground state but upon heating becomes superfluid due to entropy associated with non-topological phase fluctuations. We also discussed that such systems can have upper and lower characteristic critical superfluid velocities.

We thank B. Svistunov and N. Prokof'ev for discussions. This work was supported by the Knut and Alice Wallenberg Foundation through a Royal Swedish Academy of Sciences Fellowship, by the Swedish Research Council, and by the US National Science Foundation under the CAREER Award DMR-0955902. The computations were performed using resources provided by the Swedish National Infrastructure for Computing (SNIC) at the National Supercomputer Center in Linköping, Sweden.

¹ L. Onsager, *Il Nuovo Cimento Series 9* **6**, 249 (1949).

² C. Dasgupta and B. I. Halperin, *Physical Review Letters* **47**, 1556 (1981).

³ M. E. Peskin, *Annals of Physics* **113**, 122 (1978).

⁴ K. Fosshem and A. Sudbo, *Superconductivity: Physics and Applications* (John Wiley and Sons Ltd, 2004).

⁵ I. Herbut, *A Modern Approach to Critical Phenomena* (University press, 2007).

⁶ N. D. Mermin and H. Wagner, *Physical Review Letters* **17**, 1133 (1966).

⁷ V. L. Berezinskii, *Soviet Journal of Experimental and Theoretical Physics* **32**, 493 (1971).

⁸ V. L. Berezinskii, *Soviet Journal of Experimental and Theoretical Physics* **34**, 610 (1972).

⁹ J. M. Kosterlitz and D. J. Thouless, *Journal of Physics C Solid*

State Physics **6**, 1181 (1973).

¹⁰ E. Babaev, unpublished (2002), [arXiv:cond-mat/0201547](https://arxiv.org/abs/cond-mat/0201547).

¹¹ E. Babaev, A. Sudbo, and N. W. Ashcroft, *Nature* **431**, 666 (2004).

¹² A. B. Kuklov and B. V. Svistunov, *Physical Review Letters* **90**, 100401 (2003), [cond-mat/0205069](https://arxiv.org/abs/cond-mat/0205069).

¹³ T. K. Ng and N. Nagaosa, *Europhys. Lett.* **87**, 17003 (2009).

¹⁴ V. Stanev and Z. Tešanović, *Phys. Rev. B* **81**, 134522 (2010).

¹⁵ J. Carlstrom, J. Garaud, and E. Babaev, *Phys. Rev. B* **84**, 134518 (2011).

¹⁶ D. Weston and E. Babaev, *Phys. Rev. B* **88**, 214507 (2013).

¹⁷ S. Maiti and A. V. Chubukov, *Phys. Rev. B* **87**, 144511 (2013).

¹⁸ A. Gurevich, *Physica C Superconductivity* **456**, 160 (2007), [arXiv:cond-mat/0701281](https://arxiv.org/abs/cond-mat/0701281).